Turbulent Properties of Stationary Flows in Porous Media

Florencia Falkinhoff,[1,2,3] Alexandre Ponomarenko,[2] Jean-Lou Pierson,[1]
Lionel Gamet,[1] Romain Volk,[2] and Mickaël Bourgoin[2]
[1]IFP Energies Nouvelles, 69360 Solaize, France
[2]Ens de Lyon, CNRS, Laboratoire de physique, F-69342 Lyon, France
[3]Max Planck Institute for Dynamics and Self-Organization, Göttingen, Germany

(Received 21 July 2023; revised 29 February 2024; accepted 28 March 2024; published 22 April 2024)

In this study, we investigate the flow dynamics in a fixed bed of hydrogel beads using particle tracking velocimetry to compute the velocity field in the middle of the bed for moderate Reynolds numbers ($\mathrm{Re} = [124, 169, 203, 211]$). We discover that even though the flow is stationary at the larger scales, it exhibits complex multiscale spatial dynamics reminiscent of those observed in classical turbulence. We find evidence of the presence of an inertial range and a direct energy cascade, and are able to obtain a value for a "porous" Kolmogorov constant of $C_2 = 3.1 \pm 0.3$. This analogy with turbulence opens up new possibilities for understanding mixing and global transport properties in porous media.

DOI: 10.1103/PhysRevLett.132.174001

Flows in porous media are crucial in a wide variety of natural and industrial systems. These include for instance oil and gas extraction from underground wells through porous rocks, cooling of nuclear plants, and chemical reactions such as catalysis in packed bed reactors and separation processes [1,2]. They also play a major role in new clean energy developments [3,4], biological flows, and bioengineering applications [5–7], etc...

Understanding the hydrodynamics of flows in such situations, and its impact on mass and heat transport phenomena, is therefore of primary importance in many scientific fields and applications. The question is particularly complex when the flow in the porous bed is inertial, namely when its Reynolds number, defined below, is significantly larger than 1. This results in the emergence of a variety of intricate structures [8,9] developing at the scale of each pore (see Fig. 1) and impacting the global transport properties at play. At first sight, this complexity shares qualitative similarities with the properties of turbulence in homogeneous fluids, where the multiscale dynamics is crucial to the mixing and transport efficiency of turbulent flows.

Figure 1 shows a typical long-time exposure image of the flow recorded in our experiment (details will be given below). The flow shows a clear spatial complexity, with shear zones and strain, rotation dominated structures, stagnation points, etc., which recall the characteristic multiscale structures of a turbulent flow. Even if the flow remains essentially steady in time, as discussed below, this spatial multiscale behavior is reminiscent of the energy cascade phenomenology in turbulent flows. A direct energy cascade in turbulence occurs when the mechanical energy injected into a flow is transferred from the injection scale (L) down to the viscous dissipative scale (η). The range of scales $\eta \ll r \ll L$ is the so-called *inertial range* of turbulence. Following Kolmogorov's phenomenology (hereafter referred to as K41) [10,11] where this process is formulated in a self-similar description, the random multiscale

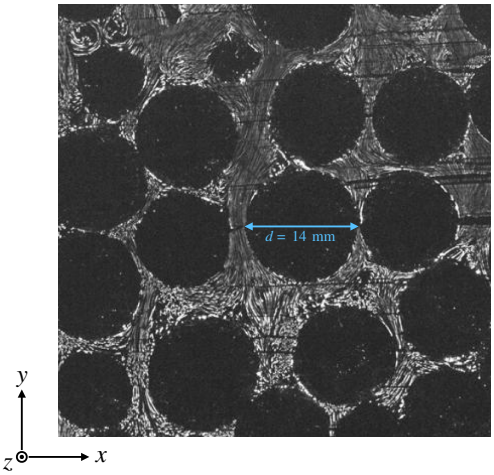

FIG. 1. Long-time exposure of a generic experiment. The tracer particles are shown in grays, and the hydrogel beads are the empty spaces in the middle. The Lagrangian dynamics is not trivial and is observed at the local scale. It is reflective of the complex nature of the system.

dynamics of turbulence is classically described in terms of the Eulerian velocity structure functions, defined as the statistical moments of the velocity increments, $\delta_r \mathbf{u} = \mathbf{u}(\mathbf{x}+\mathbf{r},t) - \mathbf{u}(\mathbf{x},t)$ between points of the flow separated by a distance $r = |\mathbf{r}|$. K41 predicts that within inertial scales, the structure functions should scale as $S_p(r) = \langle |\delta_r \mathbf{u}|^p \rangle \propto (\epsilon r)^{p/3}$, for r within the inertial range, ϵ is the energy injection-dissipation rate per unit mass, and $\langle\rangle$ denotes the ensemble average.

In this Letter, we show to which extent the spatial complexity of this steady porous medium flow shares quantitative similarities with turbulence. For that purpose we analyze transitional flows (i.e., flows that are neither laminar nor turbulent; see Ref. [12]) in porous media with the statistical tools of turbulence to characterize the spatial fluctuations of velocity and their correlations. In particular, we focus on second- and third-order statistics, whose physical relevance is fundamental as they relate respectively to the distribution of energy across scales and to the direction of the energy flux across scales. Our experiments and analysis reveal striking similarities with "classical" fluid turbulence, as the multiscale Eulerian dynamics extracted from the porous media flow are found to be virtually indistinguishable from that of homogeneous fluid turbulence.

In order to explore the hydrodynamics in the core of a porous medium, we studied the local flow in a fixed bed made of spherical particles contained in a cylinder of diameter $D = 9$ cm and height $H = 40$ cm. To be able to measure inside the pores we deployed state-of-the art particle tracking velocimetry (PTV) using index-matched hydrogel beads of mean diameter $d = 1.4$ cm to make the porous bed, where small fluorescent tracer particles are seeded into the fluid and tracked in 3D with two high-speed cameras.

More specifically, the setup, schematized in Fig. 2, consists of a closed water loop circuit, and the porous bed of hydrogel beads is fixed in a cylindrical vessel made of plexiglass with the aid of two grids at the top and bottom of the test section preventing the fluidization of the bed. A centrifugal pump is used to drive the flow of filtered water, at a constant flow rate Q which can be accurately prescribed with a solenoid valve. The flow rate is monitored by a magnetic flow meter, which provides a direct measurement of the mean superficial velocity through the bed, $U = 4Q/(\pi D^2)$. This is used to define the Reynolds number $\mathrm{Re} = Ud/\nu$ of the flow, where $\nu = 10^{-6}\,\mathrm{m}^2.\mathrm{s}^{-1}$ is the kinematic viscosity of water. It is worth noting that this election of the Reynolds number is one of the many used in porous media, as detailed in [12]. We studied the local flow at four different Reynolds numbers: $\mathrm{Re} = [124, 169, 203, 211]$. The flow at these Reynolds is found to remain steady without any signature of temporal fluctuations [12]. The saturating water is seeded with (27–35) μm polyethylene microspheres that act as tracer

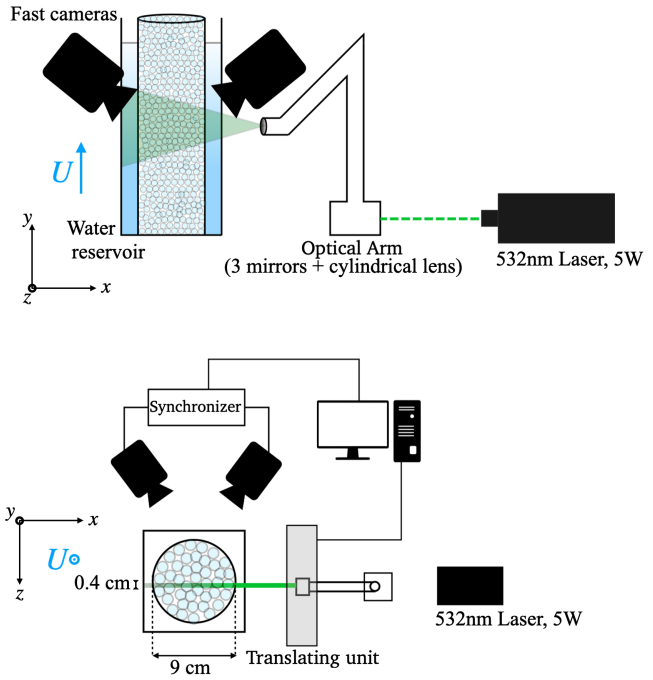

FIG. 2. Schematic representation of the experimental setup.

particles (density 0.995g/cc), and whose motion is recorded by two *Phantom v12* high-speed cameras, which were used to record several two-second films at 2200 fps and using a 12-bit, 880 × 896 px resolution. The illuminating system consists of a 5 W laser with a 532 nm wavelength. The beam enters through a light-guiding arm (*Dantec Dynamics*) that has an internal alignment mirror system, and at the end of the arm the beam is shaped into a thick fixed sheet parallel to the flow rate generated by a cylindrical lens. This gives a visualization region of approximately $(5 \times 5 \times 0.4)$ cm^3 (length × width × depth), which in terms of the hydrogel diameter is $(3.6 \times 3.6 \times 0.3)d^3$. In order to avoid any undesired reflections caused by the cylindrical shape of the bed, a rectangular vessel filled with filtered water surrounded the bed. Further details can be found in [13]. As shown in Fig. 2, the flow is driven in the y direction, and the xz plane is perpendicular to the streamwise direction (see Fig. 1 for reference), while the laser sheet is parallel to the xy plane. We note that due to the small stereoscopic angle between the two cameras of our PTV system, measurements in the y (streamwise) and x (transverse) directions have a greater spatial redundancy than the z (depth) component. As a consequence, positions recorded in the z component tend to be noisier, leading to slightly less accurate estimates of Lagrangian velocity and acceleration along this component. Therefore, given the global symmetry of our setup, all statistical quantities for the z component will be considered to be identical to those for the x component, resulting in a 3D2C PTV analysis.

In order to explore the statistical multiscale spatial properties in the present porous medium flow and possible

turbulentlike signatures, we analyze the tracer dynamics at the light of the tools typically used in turbulence. In particular, we investigate the two-point statistical properties of velocity fluctuations, defined as $u_i' = u_i - \langle u_i \rangle$, with the average done over all the trajectories obtained with the PTV.

We first emphasize the quasisteadiness of the flow which does not exhibit any major signature of temporal fluctuations. As shown in the Supplemental Material [14], the overall rate of temporal variability of the velocity at any point within the flow remains below 15% of the global spatiotemporal fluctuations. This means that the temporal variability of the trajectories is small and that most (more than 85%) of the variability of the reported velocity fluctuations arises from the spatial structure of the flow. This is drastically different from classical fluid turbulence, which is intrinsically driven by spatiotemporal fluctuations of equivalent magnitude. We call this situation *quasifrozen turbulence*.

We then compute the large scale properties of the flow and calculate the integral correlation length L. To this end, we make use of the Eulerian autocorrelation tensor, $\mathcal{R}_{ij}(r) = \langle u_i'(\mathbf{x}+\mathbf{r}) u_j'(\mathbf{x}) \rangle$ (details on the streamwise, transversal, and crossed correlation functions are shown in [14]). The correlation lengths in the transversal (x) and streamwise (y) directions are given by $L_i = \lim_{r\to\infty} \int_0^r \mathcal{R}_{ii}(\tilde{r}) d\tilde{r}/\sigma_{u_i}^2$, with $i = x$ and $i = y$ respectively and σ_{u_i} the standard deviation of the ith component of the velocity. Figure 3 (left) shows—for the streamwise component, but the conclusion holds also for the transversal one—that an asymptotic limit of the cumulative integral in this definition is well converged for all experiments at all the Reynolds numbers we investigated.

It is worth noting that L_x tends to decrease with Re whereas the opposite trend is observed for L_y, as shown in Fig. 3 (right). Overall, the large scale correlations of velocity fluctuations are characterized by transverse and streamwise integral scales which (i) are of the order of one tenth of the particle diameter, (ii) are Reynolds-dependent, and (iii) have a trend to become isotropic as Re increases (with $L_x/L_y \to 1$).

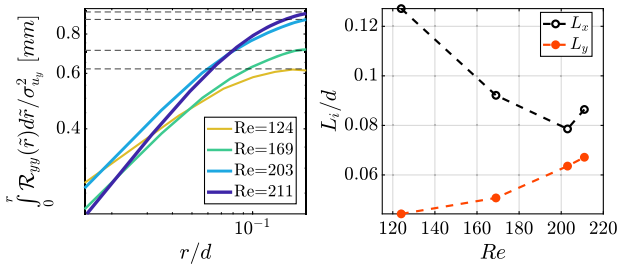

FIG. 3. Left: Cumulative integral of the correlation function $\mathcal{R}$. The plateau (horizontal dashed lines) allows us to compute L_y. Right: Integral correlation lengths calculated for the streamwise (y) and transversal (x) directions.

In order to enlarge the multiscale properties of the fluctuating velocity field, we calculate the Eulerian second-order structure function $S_2(r)$ of streamwise and transversal components.

Figure 4 shows $S_2(r)$ calculated for the streamwise component of the velocity u_y' and for the transversal component u_x', S_{2_y} and S_{2_x} respectively. Remarkably, for all the investigated Re, they both show a clear $r^{2/3}$ power law over almost one decade of scales, from the smallest resolved scale (of the order of $0.02d$) and up to $r \approx 0.2d$, which is of the order of magnitude of the calculated integral length scale. This reveals a local spatial flow dynamics where energy is distributed across scales in a strikingly similar way as it would in a turbulent flow. At larger scales $S_{2_{x,y}}$ reach a plateau at the asymptotic value of $2\sigma_{u_{x,y}}^2$ as expected for uncorrelated large scale dynamics.

Although highly appealing, the existence of a turbulent-like $r^{2/3}$ power law for S_2 is not sufficient to claim the existence of an inertial cascade (where energy is not simply distributed across scales, but actually flows across scales). The existence of a direct (where energy flows from large to small scales at the rate of ϵ per unit mass and unit time) energy cascade is indeed typically related to the Eulerian third-order structure function and the celebrated Kolmogorov's "4/5th law," $S_3^{\parallel}(r) = \frac{4}{5}\epsilon r$ [11] (with $S_3^{\parallel}$ the longitudinal third-order structure function). Given the Lagrangian nature of the original dataset recorded in our setup, we use here a mathematically equivalent relation, based on the crossed velocity—acceleration structure function $S_{au}(r) = \langle \delta\mathbf{a} \cdot \delta\mathbf{u} \rangle$. Indeed, it can be shown that for a locally homogeneous and isotropic turbulent flow [15–17],

$$S_{au}(r) = \langle \delta\mathbf{a} \cdot \delta\mathbf{u} \rangle = -2\epsilon. \tag{1}$$

In this relation the *minus* sign is characteristic of a direct energy cascade. $S_{au}(r)$ therefore yields information about the energy cascade by (i) its sign and (ii) its absolute value 2ϵ, which is expected to be constant across inertial scales and to give a direct estimate of the energy transfer rate ϵ

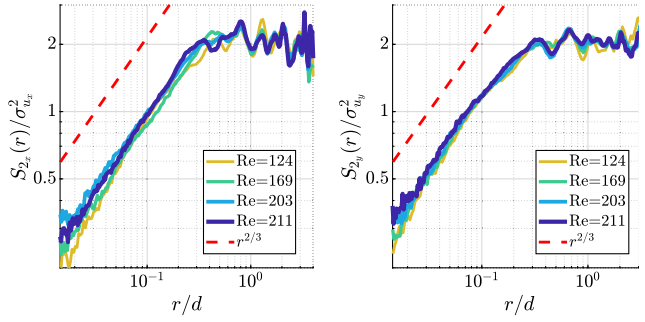

FIG. 4. Second-order structure functions for each velocity component. A two-thirds scaling (compared in dashed lines) is evident at the small scales $dr < 0.2d$.

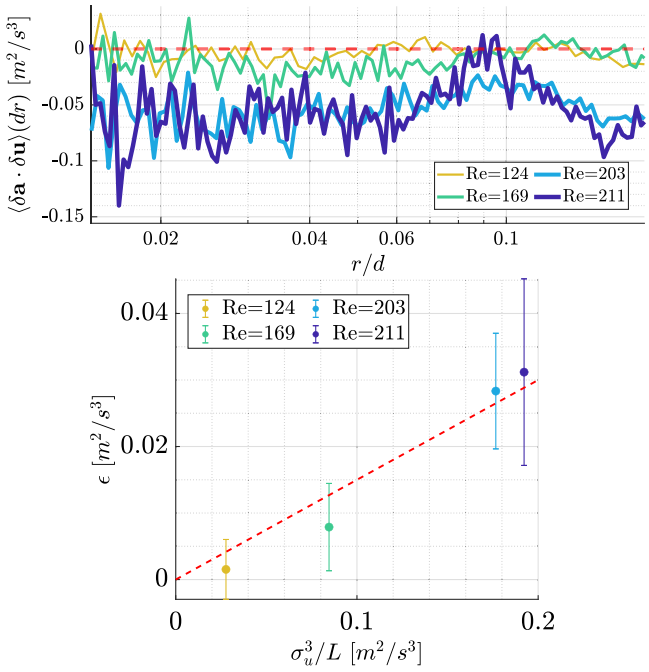

FIG. 5. Top: The acceleration-velocity structure function, which is supposed to remain constant in a homogeneous and isotropic turbulent flow, and its negative sign indicates the direction of the energy cascade. Bottom: Averaged energy dissipation rate as a function of σ_u^3. The dashed red line shows Eq. (2).

(which in stationary conditions equals the energy injection and the energy dissipation rate).

We calculated S_{au} from the y and x components only, assuming perfect isotropy between the transversal coordinates x and z, which is a reasonable assumption given the cylindrical symmetry of our experiment. We therefore estimate $\langle \delta \mathbf{a} \cdot \delta \mathbf{u} \rangle = 2\langle \delta a_x \delta u_x \rangle + \langle \delta a_y \delta u_y \rangle$.

Figure 5 (top) shows the results for the experiments at different Re. It is first observed that in spite of some scatter S_{au} remains relatively constant over the range of scales r where the $r^{2/3}$ scaling was observed for S_2. Besides, it keeps a persistent negative sign in that range, especially in the higher Re flows. In the spirit of classical turbulence, this would be associated to the presence of a direct energy cascade at inertial scales.

Using relation (1) as a formal analogy to the turbulent energy cascade, we can calculate the value of the equivalent rate of energy transfer across scales ϵ from the mean value of the plateau of S_{au}, so that $\epsilon = -\overline{\langle S_{au} \rangle}/2$ (in this case, the second average $\bar{\cdot}$ is done over r). From this estimate, we can compute several important parameters classically used to characterize turbulence by (i) Exploring at large scales the classical turbulent relation between σ_u, energy injection rate ϵ, and integral scale L:

$$\epsilon = \frac{C_\epsilon \sigma_u^3}{L}, \tag{2}$$

where C_ϵ is a nonuniversal constant typically in the range $C_\epsilon \in [0.5; 1]$ in turbulence [18]. Subsequently, the value of C_ϵ then allows one to estimate the "Taylor based Reynolds number," R_λ, of the flow, which is commonly used to characterize the intensity of turbulence. (ii) Determining the equivalent Kolmogorov—or dissipation—scale of the flow $\eta = (\nu^3/\epsilon)^{1/4}$. (iii) Determining the equivalent of the Kolmogorov constant C_2 for the second order structure function $S_2(r) = C_2(\epsilon r)^{2/3}$.

Regarding the first point, Fig. 5 (bottom) shows the energy transfer rate ϵ estimated from the energy cascade, relation (1), at inertial scales as a function of σ_u^3/L [here we defined $\sigma_u = \sqrt{[(2\sigma_{u_x}^2 + \sigma_{u_y}^2)/3]}$ and $L = 1/3(2L_x + L_y)$]. Within error bars, the trend is found to follow the same relation (2) as in classical turbulence, with $C_\epsilon = 0.15 \pm 0.05$.

We can then estimate $R_\lambda = \sqrt{\sigma_u L/\nu C_\epsilon}$ [19]. The corresponding values are shown in Table I. As it could be expected, R_λ increases with Re, although R_λ increases only 15% when Re increases more than 50%. In classical turbulence, such values ($R_\lambda \approx 80$) would be qualified as moderately turbulent, and are for instance produced in wind tunnel experiments [20]. The small variation observed for R_λ suggests that the turbulence that develops in the porous medium weakly depends on the superficial velocity driving the flow.

The energy injection rate also allows us to estimate the expected low bound of the inertial range, namely the Kolmogorov length scale $\eta = (\nu^3/\epsilon)^{1/4}$. The values obtained are shown in Table I. As it could be expected, they decrease when Re and ϵ increase, indicating that smaller scales emerge as the energy injection and the turbulence increase, following the classical phenomenology of the turbulent energy cascade.

Finally, by fitting the inertial scaling $S_2(r) = C_2(\epsilon r)^{2/3}$, the estimate of ϵ allows one to determine the equivalent of the Kolomogorov constant C_2 for the present turbulentlike dynamics (see Ref. [14]). Note that we define here C_2 based on the total second-order structure function. The corresponding values are given in Table I, showing that, within error bars, a unique value of $C_2 = 3.1 \pm 0.3$ reasonably describes the inertial range energy distribution for all values of the superficial Reynolds number explored. This value is about 2.5 times smaller than the generally accepted value

TABLE I. Different turbulent parameters calculated in terms of the energy injection rate ϵ.

Re	ϵ [m^2.s^{-3}]	η [μ]m	R_λ	C_2
124	$(1.50 \pm 0.45) \times 10^{-03}$	161 ± 12.1	71	3.5 ± 0.3
169	$(7.90 \pm 0.66) \times 10^{-03}$	106 ± 22.2	73	2.8 ± 0.3
203	$(2.83 \pm 0.87) \times 10^{-02}$	77 ± 5.93	80	3.0 ± 0.3
211	$(3.12 \pm 1.42) \times 10^{-02}$	75 ± 8.44	84	3.2 ± 0.3

for homogeneous isotropic fluid turbulence (for which $C_2 = 11C_2^{\parallel}/3$, with $C_2^{\parallel} \approx 2.1$ as the Kolmogorov constant for the longitudinal second-order structure function).

To summarize, we have investigated the flow developing in a fixed bed of hydrogel beads and found that, even though the flow is globally stationary, it develops a spatial multiscale dynamics which shares striking analogies with classical fluid turbulence.

In particular, we have shown the existence of a direct energy cascade, with a typical energy injection scale L commensurate with the pore scale and a characteristic energy transfer rate across scales ϵ. At the large scales the classical turbulent relation $\epsilon = C_\epsilon \sigma_u^3/L$ is verified. At inertial scales, the energy distribution follows the classical Kolmogorovian scaling $S_2 = C_2(\epsilon r)^{2/3}$. Although the claim of their universality will require further experiments, both parameters C_ϵ and C_2 were found to be reasonably constant, hence giving a consistent parametrization of fluctuations at large and inertial scales over the range of Reynolds numbers explored here.

These results open several interesting perspectives, for porous media physics and beyond. First, regarding porous media, the analogy with turbulence may help to build new approaches for their mixing and global transport properties. Indeed, the capacity of turbulent flows to disperse substances and fields is intimately related to the inertial multiscale dynamics [21].

Secondly, our results show that, to some extent, such transitional porous media flows can be considered as a true experimental model of frozen turbulence [22] where the underlying velocity field does not vary in time but has a rich spatial multiscale dynamics. As such, this system may help to disentangle the intricate role of spatial and temporal fluctuations occurring in real turbulence and its impact on the energy cascade and subtle phenomena such as pair dispersion and small-scale intermittency.

Finally, our findings enrich the class of out-of-equilibrium systems exhibiting a Kolmogorovian-like energy cascade, in a comparable way to what was recently reported for active matter [23]. Building such bridges between apparently disconnected phenomena for which no generic theoretical framework has yet emerged may be crucial to identifying the key common ingredients for their understanding.

[1] G. D. Wehinger, T. Eppinger, and M. Kraume, Chem. Eng. Sci. **122**, 197 (2015).
[2] P. Trogadas, M. M. Nigra, and M.-O. Coppens, New J. Chem. **40**, 4016 (2016).
[3] J. Banks and N. B. Harris, Geothermics **76**, 74 (2018).
[4] Z. Chen, K. O. Kirlikovali, K. B. Idrees, M. C. Wasson, and O. K. Farha, Chem **8**, 693 (2022).
[5] K. H. Jensen, K. Berg-Sørensen, H. Bruus, N. M. Holbrook, J. Liesche, A. Schulz, M. A. Zwieniecki, and T. Bohr, Rev. Mod. Phys. **88**, 035007 (2016).
[6] M. Peyrounette, Y. Davit, M. Quintard, and S. Lorthois, PLoS One **13**, e0189474 (2018).
[7] H. A. Santos, Biomatter **2**, 237 (2012).
[8] V. A. Patil and J. A. Liburdy, Phys. Fluids **25**, 043304 (2013).
[9] S. V. Apte, T. Oujia, K. Matsuda, B. Kadoch, X. He, and K. Schneider, J. Fluid Mech. **937**, A9 (2022).
[10] A. N. Kolmogorov, Proc. R. Soc. Lond. **434** (1991).
[11] U. Frisch, *Turbulence: The Legacy of A. N. Kolmogorov* (Cambridge University Press, Cambridge, England, 1995).
[12] B. D. Wood, X. He, and S. V. Apte, Annu. Rev. Fluid Mech. **52**, 171 (2020).
[13] F. Falkinhoff, Inertial flows in wall-bounded porous media: From pore- to global scales, Ph.D. thesis, Ecole Normale Supérieure de lyon—ENS LYON (2023).
[14] See Supplemental Material at http://link.aps.org/supplemental/10.1103/PhysRevLett.132.174001 for more details on the stationarity of the flow, correlation functions, typical pore scale structure and Kolmogorov's constant.
[15] J. Mann, S. Ott, and J. S. Andersen, *Experimental Study of Relative, Turbulent Diffusion* (Risø National Laboratory, Roskilde, 1999).
[16] S. Ott and J. Mann, J. Fluid Mech. **422**, 207 (2000).
[17] R. J. Hill, J. Turbul. **7**, N43 (2006).
[18] J. C. Vassilicos, Annu. Rev. Fluid Mech. **47**, 95 (2015).
[19] S. B. Pope, *Turbulent Flows* (Cambridge University Press, Cambridge, England, 2000).
[20] R. Monchaux, M. Bourgoin, and A. Cartellier, Phys. Fluids **22**, 103304 (2010).
[21] M. Bourgoin, J. Fluid Mech. **772**, 678 (2015).
[22] D. Schlipf, D. Trabucchi, O. Bischoff, M. Hofsäß, J. Mann, T. Mikkelsen, A. Rettenmeier, J. J. Trujillo, and M. J. Kühn, *15th International Symposium on Boundary Layer Remote Sensing* (ISARS, Paris, 2011).
[23] M. Bourgoin, R. Kervil, C. Cottin-Bizonne, F. Raynal, R. Volk, and C. Ybert, Phys. Rev. X **10**, 021065 (2020).